Validation Study of Image-Based Fractional Flow Reserve During Coronary Angiography

Mariano Pellicano, MD; Ifat Lavi, PhD; Bernard De Bruyne, MD, PhD; Hana Vaknin-Assa, MD; Abid Assali, MD; Orna Valtzer, DMD; Yonit Lotringer, MSc; Giora Weisz, MD; Yaron Almagor, MD; Panagiotis Xaplanteris, MD, PhD; Ajay J. Kirtane, MD, SM; Pablo Codner, MD; Martin B. Leon, MD; Ran Kornowski, MD

Background—Fractional flow reserve (FFR), an index of the hemodynamic severity of coronary stenoses, is derived from invasive measurements and requires a pressure-monitoring guidewire and hyperemic stimulus. Angiography-derived FFR measurements (FFR_{angio}) may have several advantages. The aim of this study is to assess the diagnostic performance and interobserver reproducibility of FFR_{angio} in patients with stable coronary artery disease.

Methods and Results—FFR_{angio} is a computational method based on rapid flow analysis for the assessment of FFR. FFR_{angio} uses the patient's hemodynamic data and routine angiograms to generate a complete 3-dimensional coronary tree with color-coded FFR values at any epicardial location. Hyperemic flow ratio is derived from an automatic resistance-based lumped model of the entire coronary tree. A total of 203 lesions were analyzed in 184 patients from 4 centers. Values derived using FFR_{angio} ranged from 0.5 to 0.97 (median 0.85) and correlated closely (Spearman ρ=0.90; P<0.001) with the invasive FFR measurements, which ranged from 0.5 to 1 (median 0.84). In Bland–Altman analyses, the 95% limits of agreement between these methods ranged from −0.096 to 0.112. Using an FFR cutoff value of 0.80, the sensitivity, specificity, and diagnostic accuracy of FFR_{angio} were 88%, 95%, and 93%, respectively. The intraclass coefficient between 2 blinded operators was 0.962 with a 95% confidence interval from 0.950 to 0.971, P<0.001.

Conclusions—There is a high concordance between FFR_{angio} and invasive FFR. The color-coded display of FFR values during coronary angiography facilitates the integration of physiology and anatomy for decision making on revascularization in patients with stable coronary artery disease.

Clinical Trial Registration—URL: https://www.clinicaltrials.gov. Unique identifier: NCT03005028.

(*Circ Cardiovasc Interv*. 2017;10:e005259. DOI: 10.1161/CIRCINTERVENTIONS.116.005259.)

Key Words: angiography ■ catheterization ■ microcirculation ■ tomography ■ workflow

Fractional flow reserve (FFR) is a physiological index that quantifies the hemodynamic impact of epicardial atherosclerotic stenoses. It is defined as the ratio of hyperemic myocardial flow in the presence of stenosis, to the hyperemic flow in its absence, and is obtained by measuring the ratio of distal coronary pressure and the aortic pressure, respectively, using pressure-measuring guidewires during maximal hyperemia.[1–3] FFR is considered the standard of reference for clinical decision making, particularly of angiographically indeterminate coronary lesions. Clinical outcome studies have shown that for nonsignificant lesions (FFR >0.80), medical therapy should be preferred, whereas in cases of significant stenoses (FFR ≤0.80), coronary revascularization should be considered.[4–11] Accordingly, both the US and European guidelines recommend using FFR to guide the treatment strategy in stable coronary lesions.[12,13]

See Editorial by Morris and Gunn

Nevertheless, for a variety of practical reasons, FFR measurements remain underused. Therefore, the ability to derive FFR values from routinely performed coronary angiograms, without the need for a pressure guidewire or hyperemic stimulus, could have an important impact on daily clinical practice by streamlining the workflow within the catheterization laboratory and avoiding the need for invasive coronary measurements.[14–16]

Several image-based FFR methodologies have recently been introduced. Computational fluid dynamics (CFD) simulation applied to cardiac computed tomographic images and

Received March 13, 2017; accepted July 17, 2017.

From the Cardiovascular Center Aalst, OLV Hospital, Belgium (M.P., B.D.B., P.X.); Rabin Medical Center, Petach Tikva, Israel (I.L., H.V.-A., A.A., O.V., P.C., R.K.); Department of Advanced Biomedical Sciences, Federico II University of Naples, Italy (M.P.); CathWorks Ltd, Ra'anana, Israel (I.L., O.V., Y.L.); Columbia University Medical Center, New York-Presbyterian Hospital (A.J.K., P.C., M.B.L.); and Shaare Zedek Medical Center, Jerusalem, Israel (G.W., Y.A.).

The Data Supplement is available at http://circinterventions.ahajournals.org/lookup/suppl/doi:10.1161/CIRCINTERVENTIONS.116.005259/-/DC1.

Correspondence to Bernard De Bruyne, MD, PhD, Cardiovascular Center Aalst, OLV-Clinic, Moorselbaan, 164, B-9300 Aalst, Belgium. E-mail bernard.de.bruyne@olvz-aalst.be

WHAT IS KNOWN

- Fractional flow reserve (FFR) is the gold standard for hemodynamic assessment of coronary intermediate stenoses but remains underused because of its invasive nature.
- Several image-based FFR methodologies exist that are based on computational fluid dynamics simulation.
- FFR_{angio} uses routine angiograms to generate a complete 3-dimensional coronary tree with color-coded FFR values at any epicardial location, without the need of a pressure wire or hyperemic stimulus or the need of computational fluid dynamics simulation.

WHAT THE STUDY ADDS

- This multicenter study on >200 lesions demonstrates the diagnostic accuracy of FFR_{angio}, which has a high sensitivity and specificity when compared with invasive FFR.
- FFR_{angio} is unique in that it provides a comprehensive physiological assessment of the entire coronary tree within minutes, enabling online FFR measurement during the angiographic procedure.

to flat detector angiograms for the evaluation of noninvasive FFR have been proposed.[14,16–21] However, the computational complexity of such simulations requires manual interaction and considerable processing time, which limits the application of these approaches in clinical practice. Nevertheless, these methods have shown that computer-based techniques are able to assess the hemodynamic significance of coronary lesions, emphasizing the potential of noninvasive FFR measurements in the catheterization laboratory.

FFR_{angio} (developed by CathWorks, Ltd) provides a 3-dimensional (3D) functional angiography mapping of the coronary tree with superimposed, color-coded, FFR values. Stated another way, FFR_{angio} displays a functional angiogram. This computational method is based on a rapid flow analysis after a classification of the dynamic characteristics of the vessels in conjunction with the patient's hemodynamic information, allowing to assess FFR using routine angiograms within a few minutes of automatic processing. All stenoses are converted into resistances in a lumped model, whereas scaling laws[22–24] are used to estimate the microcirculatory bed resistance. The FFR values at each point along each vessel are calculated from the ratio of hyperemic flow rates in the stenosed vessel versus the healthy vessel trees.

In the present report, we describe the theoretical basis and the practicalities of FFR_{angio}, as well as its diagnostic accuracy and interobserver reproducibility compared with invasive FFR.

Methods

FFR_{angio}

The primary element of FFR_{angio} is the proprietary 3D rebuild of the coronary tree from 2-dimensional (2D) images. This is accomplished automatically by reconstructing the geometry of the tree, including its centerlines and cross-sections at each point along them, as well as the exact topology. The reconstruction is based on the known geometry of ≥3 projections from single-plane angiograms and uses epipolar ray tracing (Figure 1) together with mathematical constraints enforcing the tree's structure. The system is able to construct each vessel separately such that each region/branch/lesion is not necessarily reconstructed from the same views, yet at the same time the tree topology is preserved and adheres to that reflected in all of the 2D images. A self-validation step follows whereby the 3D shape of the coronary arteries is projected back onto the 2D images used in its recovery, allowing for this verification loop to be inspected by the user. Finally, the 3D engine contains a compensation mechanism, whereby it uses all available projections at once to compensate for the different x/y/z displacements apparent in the breathing and patient movements. In addition, panning of the table and C-arm is not recommended during the cine acquisition.

Several studies have described the use of stereo-geometry to recover 3D coronary shape.[25–28] However, the uptake of the available technologies has been limited because of a low cost effectiveness and perceived value versus effort. It is, therefore, critical to reconstruct the 3D tree in an automatic fashion, with only minimal manual effort required to guide the processing. To achieve this, iterative multiplane ray tracing is repeatedly performed in FFR_{angio} to recover the spatial position of the vessel nodes while compensating for breathing, table motion, and uneven cardiac cycle phase shifts.

Main vessels and side vessels (up to the first or second generation) must preserve the correct connectivity, stemming from the 2D projections. Segment-node representation is maintained, whereas uneven motion displacements are compensated for using iterated-closest-point alignment.

The coronary tree, represented by position and diameter values for all vessels, can then be surfaced using a triangular mesh and rendered to display a 3D coronary model (Figure 2). Next, the system scans the entire reconstructed tree in 3D and analyzes each branch and each bifurcation (or trifurcation), looking for narrowed regions. Diameter stenosis is clinically defined as the proportion between the actual diameter of the measured vessel versus that of the healthy vessel.[29,30] An automatic stenosis analyzer, therefore, requires 3 components critical to the proper evaluation of the extent of the lesion. Because stenoses vary in length, location, and spread, it is necessary to look at each vessel at different scales. The first is at the segment level, where a segment is defined as the portion of a vessel that connects 2 junctions. The second scale is the branch level, looking at the entire vessel as a whole. Finally, as a third scale, the junction level is where a parent branch bifurcates (or trifurcates) into secondary or tertiary branches. At each level, a tailored process starts with an accurate detection of vessel walls, followed by determination of the reference diameter. It then evaluates the magnitude of flow resistance because each narrowing is added to the tree.

A hemodynamic evaluation follows, where the contribution of each narrowing to the total resistance to flow is taken into account, and a subsequent lumped model is built. The contribution to the control of flow of certain vessels depends on their impact on overall resistance. The resistance of a vessel can be readily estimated from its length and diameter, applying Poiseuille law, and neglecting entrance effects and peculiarities of rheology.[31] Applying various models to infer resistance, based on Poiseuille forces, Bernoulli forces, and the resistance model described in the study by Kirkeeide,[32] all yield equivalent accuracies of the FFR_{angio} values.

The extent of the model is such that it includes a stenosis and spreads distally as far as the resolution of the imaging modality allows. The number of bifurcations is limited by the resolution to which vascular width can be determined from the images (>0.5 mm), and the availability of a larger number of measurable bifurcations is a potential advantage for a more complete reconstruction of the detailed vascular resistance. The accumulated volume of the coronary vessels and total coronary length, calculated from a reconstruction of its geometry, enables an estimation of normal supply derived from the microcirculatory bed resistance.[22–24,33,34]

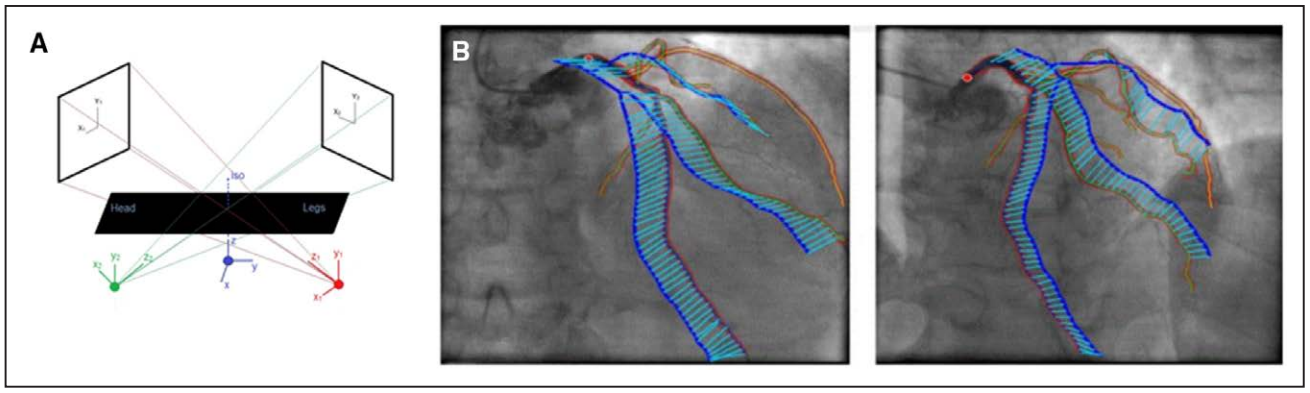

Figure 1. Three-dimensional reconstruction is based on the known geometry of ≥2 projections and uses epipolar ray tracing together with topology-preserving constraints. **A**, The epipolar geometry's frame-of-reference for 2 projections. **B**, Segment-node representation is maintained, while uneven motion displacements are compensated for.

The solution of the lumped model based on the inlet and outlet boundary conditions allows to evaluate ratios of flow rate for stenosed versus healthy coronary trees. A color-mapped mesh is then generated and displays the FFR values at every location, as long as the vessel diameter is not limited by image resolution.

Study Population

In this multicenter study, we included subjects aged ≥18 years who were diagnosed with stable angina, referred for coronary angiography, and in whom 50% to 90% diameter stenosis was present by visual estimation, and FFR measurements were performed for clinical reasons in at least 1 coronary artery. Patients with left main stenosis, ostial right coronary artery and left main stenosis, in-stent restenosis at the target vessel, previous bypass surgery, and diffuse coronary disease were excluded. In all cases, the stenosis was clearly delineated on the angiogram. The study was conducted in 2 time periods. The first one was a pilot study conducted in 2 centers (Rabin Medical Center, Petach Tikva, Israel, n=74 lesions; and Cardiovascular Center Aalst, Belgium, n=27 lesions), and the second was an extension of the first during which 2 additional centers recruited patients (Rabin Medical Center, Petach Tikva, Israel, n=31 lesions; Cardiovascular Center Aalst, Belgium, n=46 lesions; Columbia University Medical Center, New York, n=8 lesions; and Shaare Zedek Medical Center, Jerusalem, Israel, n=17 lesions). For this reason, the first 2 centers recruited more than the last 2 centers. Yet, it is important to emphasize that the algorithms and the methods were exactly the same. This report refers to the data obtained from both study stages and presents the combined analyses of all results collected. Baseline characteristics by site are available in Table I in the Data Supplement. The study protocol was approved by the Institutional Review Board or Ethics Committee at each center, and subjects gave informed consent where required.

Coronary Angiography

The diagnostic catheterization was performed using a 5F or 6F catheter according to local procedures, using either the radial or the femoral approach. After administration of intracoronary nitrates, 3 projections of the vessel to be measured were acquired at a magnification allowing visualization of the entire vessel, from proximal to most distal edge. The exact inclination of the radiographic tube was left to the operator's discretion. Care was taken to fill the artery as completely as possible with contrast medium and to image the entire coronary tree at each view. Coronary angiography cines were recorded at 15 frames per second (using AXIOM-Artis, Siemens; AlluraXper, Philips Healthcare; and Innova, GE Healthcare).

Invasive FFR Measurements

Invasive FFR measurements were performed using 6F guide catheters and a Certus Wire (Abbott, n=94 stenoses), an OptoWire (Opsens, n=9), or a Wave Wire (Philips, n=100). Hyperemia was obtained by adenosine, either by intracoronary administration (200 µg for the left coronary tree and 100 µg for the right) or by intravenous infusion (140 µg/kg per minute). Measurements obtained with adenosine intracoronary were repeated twice, and their mean value used for analyses; all tracings were stored for further review. Care was taken to document the exact anatomic position of the sensor during the invasive FFR measurements.

FFR_{angio} Computation

For this validation study, invasive FFR measurements were recorded and stored electronically and in a case record that was established immediately. In contrast, the FFR_{angio} computations were performed offline in a remote location by 2 operators not present in the catheterization laboratory, blinded to each other and to the invasive FFR results. The high-resolution Digital Imaging and Communications in Medicine files (>700*700 pixels) were stored on DVDs and shipped for off-line analyses. The FFR_{angio} software device uses dedicated hardware. Each series of Digital Imaging and Communications in Medicine cine sequences were loaded and processed along with the patient's mean aortic pressure obtained at the time of the angiogram. User interaction was required to guide automatic processing and included verification of cardiac phase synchronization and proper extraction of vessel centerlines and radii. The automatic processing consisted of the 3D tree reconstruction and the flow estimation (case examples are presented in Figure 2).

To test interobserver variability, and the possible influence of human factors on the results of FFR_{angio}, 2 independent operators analyzed all angiograms. The mean values were compared with the FFR measurements obtained with the invasive pressure wire, at the exact location of the sensor.

Statistical Approach

Standard summary statistical tests were used. The normality of measured variables was tested using the Shapiro–Wilk test. First, the consistency (absolute agreement) of the FFR_{angio} values, as measured by the 2 independent operators, was assessed with the intraclass correlation coefficient. Then, linear regression with FFR_{angio} (mean of the 2 independent operators) as the dependent variable and wire-based FFR as the predictor variable was performed, and the linear slope and intercept were calculated. To explore the agreement between invasive and noninvasive FFR estimates, Bland–Altman analyses were plotted, and the 95% limits (1.96*SD) of agreements were calculated. Estimated bias (defined as the mean difference between the 2 methods±SD) was calculated, and 1-sample *t* test was used to evaluate whether it differed significantly from zero. The receiver-operating characteristic (ROC) curve for FFR_{angio} was plotted with wire-based FFR as the gold-standard binary classifier (threshold of 0.80); the C statistics and sensitivities and specificities for different FFR_{angio} cutoff values were calculated. ROC curves for the percentage of diameter stenosis by visual estimation and for 2D quantitative coronary angiography (QCA) were similarly plotted, and C statistics of the ROC

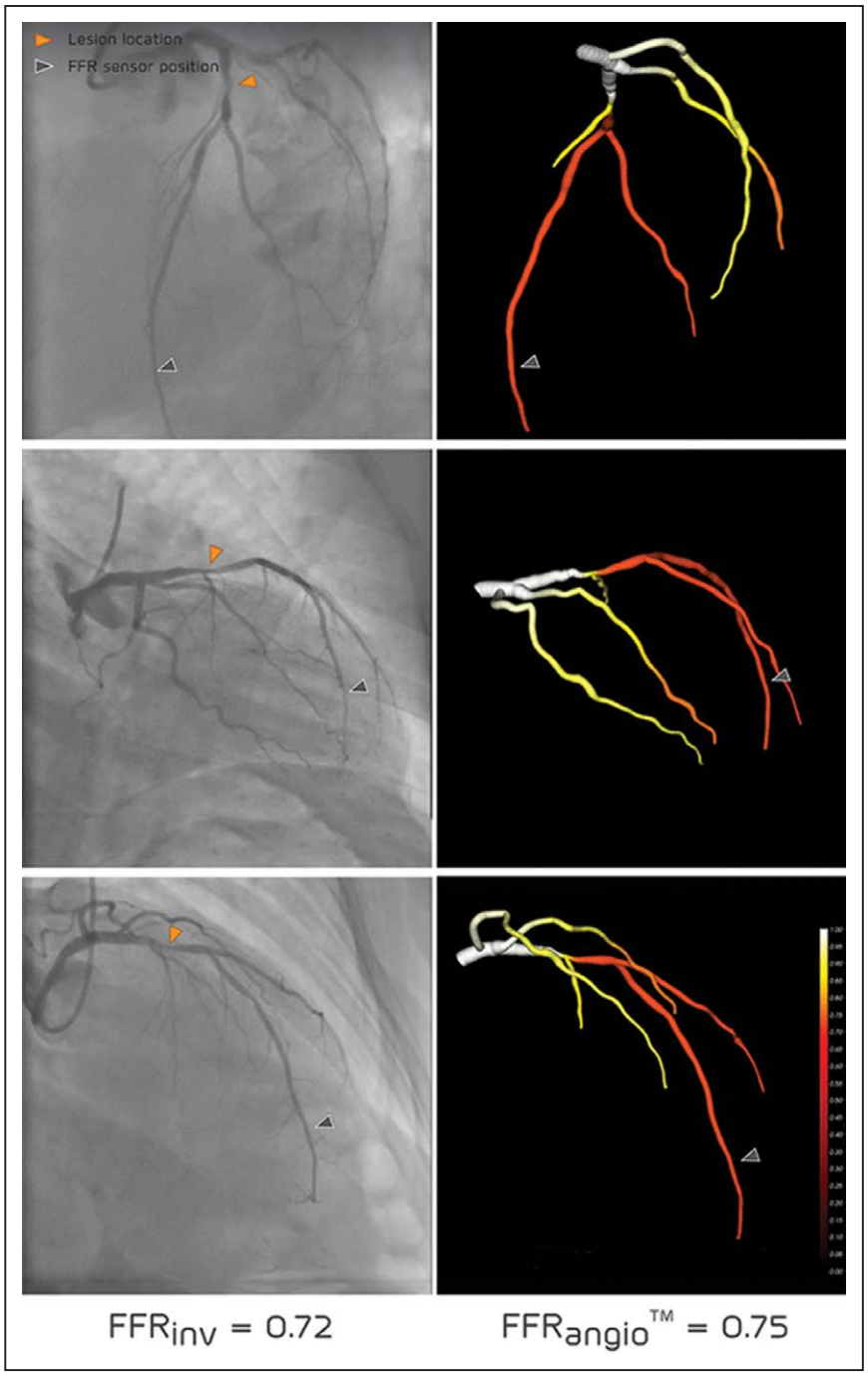

Figure 2. Left, Three orthogonal angiographic projections of the left coronary tree showing an intermediate lesion in the mid portion of the left anterior descending artery. Assessment of functional coronary lesion severity correlated well using conventional invasive fractional flow reserve (FFR) and image-derived FFR_{angio} (0.72 and 0.75; respectively). **Right**, Three-dimensional functional angiography mapping (FFR_{angio}).

curves were subsequently compared using χ^2 test. All FFR values <0.5 (n=5) were truncated to a default value of 0.50. The level of statistical significance was set at P=0.05. Statistical analyses were performed with Stata 13 and GraphPad Prism for Mac.

Results

A total of 199 patients were enrolled for the study, but analysis was performed only in 184 of them (123 men, 203 stenoses) because of protocol violation in 8 cases (eg, post coronary bypass surgery, aorto-ostial stenosis, and in-stent restenosis lesions) and inadequate quality of the angiogram in 7 patients. Baseline characteristics of all participants are presented in the Table. Lesions were distributed as follows: 118 in the left anterior descending, 30 in the left circumflex, 39 in right coronary arteries, 5 in intermediate branches, 2 in the diagonal branch, and 9 in the obtuse marginal branch. Sixty-seven percent of the invasive FFR values were between 0.70 and 0.90, and 35% between 0.75 and 0.85. FFR measurement by site is available in Table II in the Data Supplement.

The average intraclass correlation coefficient for the 2 measurements of FFR_{angio} conducted by 2 different operators blinded to each other and blinded to the results of invasive FFR was 0.962 with a 95% confidence interval from 0.95 to 0.971 (P<0.001; Figure 3).

Figure 4 shows the correlation between the mean FFR_{angio} value as the dependent variable and the wire-based FFR as the predictor variable and the corresponding Bland–Altman plots. The estimated bias was 0.007, indicating that FFR_{angio} values

Table. Baseline Characteristics of the Study Cohort

Baseline Characteristics of the Patients	
Age, mean±SD, y	65.9±9.5
Male sex, %	123/184 (67)
Family history of CAD, %	60/184 (33)
Hypertension, %	124/184 (67)
Hypercholesterolemia, %	164/184 (89)
Diabetes mellitus, %	59/184 (32)
Smoking (current), %	32/184 (17)
Smoking (prior), %	42/184 (23)
Prior MI, %	35/184 (19)
Prior PCI, %	66/184 (36)
Stable angina, %	129/184 (71)
Unstable angina %	34/184 (18)
NSTEMI, %	21/184 (11)
Radial access, %	137/184 (74)
Femoral access, %	47/184 (26)

CAD indicates coronary artery disease; MI, myocardial infarction; NSTEMI, non–ST-segment–elevation myocardial infarction; and PCI, percutaneous coronary intervention.

do not systematically underestimate or overestimate invasive FFR values. The 95% limits of agreement were −0.096 to 0.112. Visual estimation of the Bland–Altman plot indicates that the differences between the 2 methods, and the scatter around the bias line, are stable as the average increases. Linear regression per site and Bland–Altman analysis when considering only the minimum or maximum invasive FFR measurement appear in Tables III and IV in the Data Supplement.

Using 0.8 as a cutoff value for FFR_{angio} and invasive FFR, the sensitivity, specificity, diagnostic accuracy, positive likelihood ratio, and negative likelihood ratio for FFR_{angio} were 88%, 95%, 93%, 22, and 0.12, respectively.

Figure 5 shows the plots of invasive FFR values compared with FFR_{angio}, diameter stenosis by visual estimate, and diameter stenosis by quantitative coronary angiography. The corresponding areas under the respective ROC curves are 0.97, 0.57, and 0.61 (Figure I in the Data Supplement).

ROC curve analyses per hospital were made, and their C statistics were compared. The C statistics for FFR_{angio} for each site was 0.99, 0.96, and 0.90, respectively, per order of sites (P=0.22). The C statistic for one site could not be calculated because of the small number of significant lesions analyzed.

Discussion

Main Findings

In the present validation study, we compared angiography-derived FFR values using the CathWorks proprietary technology (FFR_{angio}) to simultaneously obtained invasive FFR measurements. The study included patients with typical characteristics encountered in most trials dealing with percutaneous coronary intervention, including lesions associated with a large range of FFR values (0.5–1; mean=0.81±0.11). The 95% limits of agreement were found to be between −0.096 and +0.112. When continuous FFR values were dichotomized using the standard clinical cutoff value of 0.80, FFR_{angio} achieved a diagnostic accuracy of 93%. Importantly, the fact that 67% of the lesions analyzed had invasive FFR values of 0.70 to 0.90, and 35% of the lesions had invasive FFR values between 0.75 and 0.85, that is, adjacent to the cutoff value, proves a high diagnostic accuracy for the entire clinically relevant range and not only in extreme cases. Moreover, a low interobserver variability was demonstrated for the FFR_{angio} system.

When compared with other novel FFR methodologies including angiogram-based FFR, instant wave-free ratio, and 3D fractional flow reserve computed tomography, the limits of agreements evident with FFR_{angio} are in-line and in most instances even lower. Trials on other angiographic FFR methods reported 95% confidence interval from ≈−0.15 to 0.18 (virtual FFR),[17] ≈−0.17 to 017 (fast virtual FFR),[18] and −0.12 to 0.12 (quantitative flow ratio [QFR]).[21] An analysis on instant wave-free ratio used in 1129 patients showed the 95% confidence interval to be from −0.08 to 0.26 when compared with FFR.[35] Systematic analysis of 5 large fractional flow reserve computed tomography trials (908 vessels from 536 patients) demonstrated a small bias toward underestimation of invasive FFR by fractional flow reserve computed tomography (bias, −0.029 [0.09]; P<0.001), with 95% limits of agreement ranging from −0.212 to 0.155 with a 95% confidence interval from −0.08 to +0.26.[36]

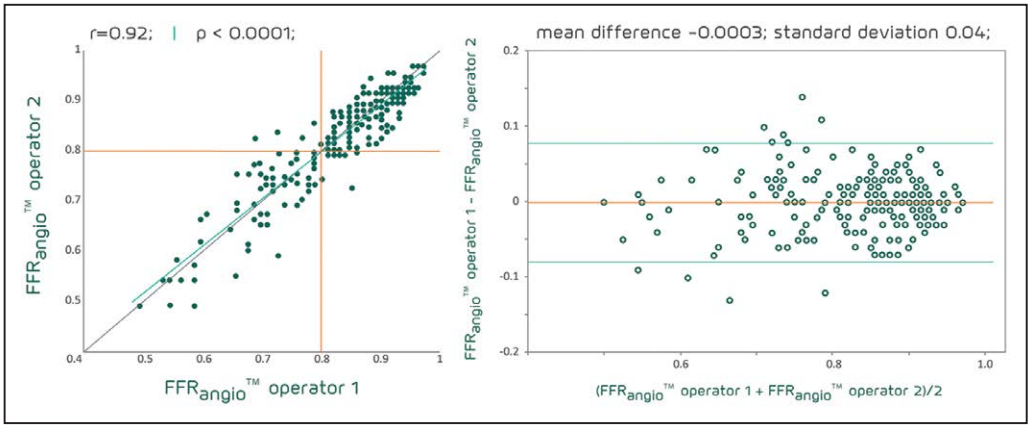

Figure 3. Correlation (scatter plot) of the FFR_{angio} values obtained by 2 blinded operators (**left**), with the corresponding Bland–Altman plot (**right**). The intraclass correlation (consistency of agreement) was found to be 0.962 (95% confidence interval, 0.950–0.971).

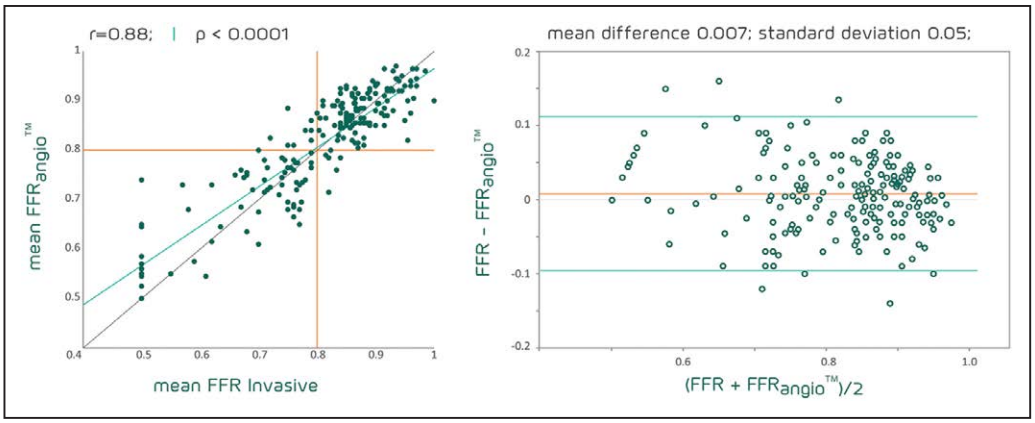

Figure 4. Correlation between invasive fractional flow reserve (FFR) and FFR_{angio} (**left**) and the corresponding Bland–Altman plot (**right**). FFR_{angio} values are the mean of 2 independent analyses performed by different observers. Invasive FFR values are the mean of 2 measurements done by the same operator.

Other Angiography-Based Methods to Derive FFR

Several groups have attempted to use angiographic data to simulate invasive FFR measurements[14,16–21] with the purpose of providing real-time physiology data in the catheterization laboratory. Morris et al[17] used a CFD method based on angiographic studies and FFR measurements in 19 patients with stable CAD, but this system requires a rotational coronary angiogram, which is not universally available; prior knowledge in CFD calculation is required; and the processing time is long.

Tu et al[21] used the QFR method derived from 3 different flow models (Medis, Leiden, the Netherlands) based on 3D QCA of vessel segments and the flow moving through the stenosis. For 84 vessels in 73 patients, the investigators reported a correlation of fixed quantitative flow ratio, contrast quantitative flow ratio, and adenosine quantitative flow ratio to invasive FFR as r=0.69, 0.77, and 0.72, respectively, and overall accuracy of 80% (fixed quantitative flow ratio), 86% (contrast quantitative flow ratio), and 87% (adenosine quantitative flow ratio). This system relies on 3D QCA combined with additional Thrombolysis in Myocardial Infarction frame count from high-quality images (30 frames per second) for the calculation of mean volumetric flow rate at hyperemia and still requires induced hyperemic conditions. In addition, this method provides assessment of the main vessel of interest without providing the side branches, and the analysis is limited to off-line computation by a core laboratory.

Tröbs et al[20] also used CFD to retrospectively calculate angiography-based FFR in 73 patients with CAD. The correlation coefficient reported was 0.85, and the diagnostic accuracy reached 90%. The model included a maximum of 1 side branch and manual correction of automatically detected vessel contours that introduced some interobserver variability. Bland–Altman analysis was 0.0082 with an SD of −0.117 to 0.134.

Papafaklis et al[18] used 3D QCA in 139 vessel segments with intermediate lesions as assessed by invasive FFR. The 3D QCA models were processed with CFD to calculate the lesion-specific pressure gradient (ΔP) and construct the ΔP-flow curve, from which the virtual functional assessment index was derived. The diagnostic accuracy of virtual functional assessment index to predict invasive FFR reached 88%.

All of these methods contribute to the continuing effort to add a physiology overlay to the base angiograms. However, to this moment, there is no commercially available solution allowing for a real-time calculation of hemodynamic measurements, and research is still needed to bring these techniques to clinical use. Large-scale studies shall follow to prove the applicability to daily practice.

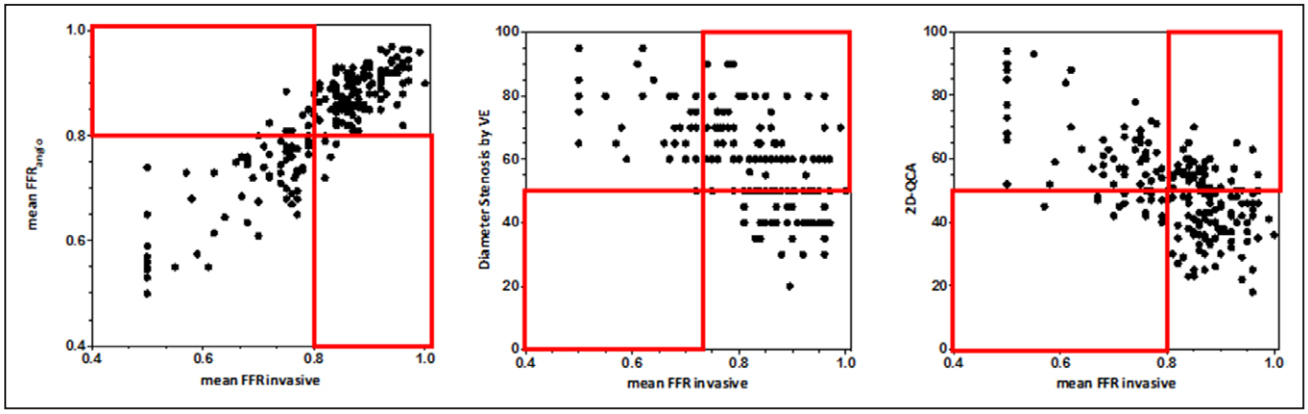

Figure 5. Plots of invasive fractional flow reserve (FFR) values compared with FFR_{angio}, diameter stenosis by visual estimate, and diameter stenosis by quantitative coronary angiography. The red borders indicate the values misclassified by FFR_{angio}, diameter stenosis by visual estimate, and diameter stenosis by quantitative coronary angiography, respectively.

Clinical Applications

The image acquisition requirements and the user interface of an image-based FFR system should be designed to harmonize with the workflow of a catheterization laboratory. To achieve this, at least 3 conditions should be met.

First, data acquisition should minimally disrupt routine angiography. FFR_{angio} only requires the acquisition of 2 to 3 conventional radiographic projections, in which the lesions can be clearly delineated. Care should be taken to visualize the entire coronary tree on the screen and to optimize filling. The acquisition angles needed for the FFR_{angio} measurements require no deviation from the routine workflow. There is no need for vasodilation, nor any approximation of coronary flow. The images should be of high resolution (≥700×700), with a frame rate of at least 10 frames per second; all these parameters are routinely available in modern catheterization suites.

Second, the processing time should be as short as possible. In the present study, this aspect could not be quantified because the FFR_{angio} processing was performed offline to ensure the blinding of the operators.

Third, the process should be as much operator independent as possible. The present version of the FFR_{angio} technology requires minimal user guidance in the flow calculation process. This is translated into a low interoperator variability.

In addition, it seems desirable to provide the physician with a full physiological roadmap, rather than only single-vessel segments. Once such a complete physiological roadmap is derived from the classical angiogram and simultaneously displayed next to it, anatomy and function can be easily integrated into the clinical decision-making process.

Also, FFR_{angio} technology and its 3D reconstruction and complete 3D QCA of the entire coronary tree allows for defining of the optimal projection for estimation of the lesion during the percutaneous coronary intervention procedure. In addition, the 3D reconstruction provided by the FFR_{angio} technology allows demonstration and assessment of the lesion from any angle.

Finally, the virtual reconstruction of the normal vessel diameters based on the reference diameters extracted during the stenosis analysis can be used to simulate stent placement and to predict anatomic and physiological outcomes.

Limitations

Many limitations have to be acknowledged. (1) All patients in this study exhibited discrete, well-delineated, stenoses. Diffuse disease, ostial lesions, and in-stent restenosis were not included. Therefore, it is now essential to test the diagnostic accuracy of FFR_{angio} in real-world consecutive patients. (2) Because the spatial resolution of the angiogram is close to the dimensions of the minimal luminal diameter in severe stenosis, the FFR_{angio} values <0.50 were truncated to 0.50. This has likely decreased the degree of correlation. Yet, in clinical practice, however, this is of little importance because decisions made on the basis of such low values will not change. (3) All FFR_{angio} measurements were done offline. While this enabled complete blinding of the readers, it does not correspond to the clinical scenario for which the measure has been developed. An online validation study is on its way. (4) The present study does not provide intraoperator variability. Yet, interobserver variability has been thoroughly studied and is expected to be larger than intraobserver variability.

Conclusions

The FFR_{angio} shows a high concordance with invasive FFR and can be obtained within minutes in the setting of a regular coronary angiogram. If confirmed in a larger study, FFR_{angio} appears as an easy means of integrating anatomy and physiology with high spatial resolution in the catheterization laboratory. This, in turn, may facilitate the adoption of FFR-based clinical decision making regarding coronary revascularization.

Sources of Funding

This study was funded by CathWorks Ltd.

Disclosures

Dr Pellicano has been supported by a research grant provided by the Cardiopath PhD program. Dr De Bruyne's institution receives consultancy fees on his behalf from Boston Scientific, St Jude Medical, and Opsens. Dr Kornowski is a cofounder at CathWorks Ltd (Ra'anana, Israel). Dr Lavi, O. Valtzer, and Y. Lotringer are employees of CathWorks. The other authors report no conflicts.

References

1. Pijls NH, van Son JA, Kirkeeide RL, De Bruyne B, Gould KL. Experimental basis of determining maximum coronary, myocardial, and collateral blood flow by pressure measurements for assessing functional stenosis severity before and after percutaneous transluminal coronary angioplasty. *Circulation*. 1993;87:1354–1367.
2. De Bruyne B, Baudhuin T, Melin JA, Pijls NH, Sys SU, Bol A, Paulus WJ, Heyndrickx GR, Wijns W. Coronary flow reserve calculated from pressure measurements in humans. Validation with positron emission tomography. *Circulation*. 1994;89:1013–1022.
3. De Bruyne B, Pijls NH, Paulus WJ, Vantrimpont PJ, Sys SU, Heyndrickx GR. Transstenotic coronary pressure gradient measurement in humans: in vitro and in vivo evaluation of a new pressure monitoring angioplasty guide wire. *J Am Coll Cardiol*. 1993;22:119–126.
4. De Bruyne B, Fearon WF, Pijls NH, Barbato E, Tonino P, Piroth Z, Jagic N, Mobius-Winckler S, Rioufol G, Witt N, Kala P, MacCarthy P, Engström T, Oldroyd K, Mavromatis K, Manoharan G, Verlee P, Frobert O, Curzen N, Johnson JB, Limacher A, Nüesch E, Jüni P; FAME 2 Trial Investigators. Fractional flow reserve-guided PCI for stable coronary artery disease. *N Engl J Med*. 2014;371:1208–1217. doi: 10.1056/NEJMoa1408758.
5. Muller O, Mangiacapra F, Ntalianis A, Verhamme KM, Trana C, Hamilos M, Bartunek J, Vanderheyden M, Wyffels E, Heyndrickx GR, van Rooij FJ, Witteman JC, Hofman A, Wijns W, Barbato E, De Bruyne B. Long-term follow-up after fractional flow reserve-guided treatment strategy in patients with an isolated proximal left anterior descending coronary artery stenosis. *JACC Cardiovasc Interv*. 2011;4:1175–1182. doi: 10.1016/j.jcin.2011.09.007.
6. Pijls NH, De Bruyne B, Peels K, Van Der Voort PH, Bonnier HJ, Bartunek J Koolen JJ, Koolen JJ. Measurement of fractional flow reserve to assess the functional severity of coronary-artery stenoses. *N Engl J Med*. 1996;334:1703–1708. doi: 10.1056/NEJM199606273342604.
7. Pijls NH, van Schaardenburgh P, Manoharan G, Boersma E, Bech JW, van't Veer M, Bär F, Hoorntje J, Koolen J, Wijns W, de Bruyne B. Percutaneous coronary intervention of functionally nonsignificant stenosis: 5-year follow-up of the DEFER Study. *J Am Coll Cardiol*. 2007;49:2105–2111. doi: 10.1016/j.jacc.2007.01.087.
8. Puymirat E, Peace A, Mangiacapra F, Conte M, Ntarladimas Y, Bartunek J, Vanderheyden M, Wijns W, De Bruyne B, Barbato E. Long-term clinical outcome after fractional flow reserve-guided percutaneous coronary revascularization in patients with small-vessel disease. *Circ Cardiovasc Interv*. 2012;5:62–68. doi: 10.1161/CIRCINTERVENTIONS.111.966937.
9. Tonino PA, De Bruyne B, Pijls NH, Siebert U, Ikeno F, van' t Veer M, Klauss V, Manoharan G, Engstrøm T, Oldroyd KG, Ver Lee PN, MacCarthy PA, Fearon WF; FAME Study Investigators. Fractional flow reserve versus angiography for guiding percutaneous coronary intervention. *N Engl J Med*. 2009;360:213–224. doi: 10.1056/NEJMoa0807611.
10. van Nunen LX, Zimmermann FM, Tonino PA, Barbato E, Baumbach A, Engstrøm T, Klauss V, MacCarthy PA, Manoharan G, Oldroyd KG, Ver Lee PN, Van't Veer M, Fearon WF, De Bruyne B, Pijls NH; FAME Study Investigators. Fractional flow reserve versus angiography for guidance of PCI in patients with multivessel coronary artery disease (FAME): 5-year

follow-up of a randomised controlled trial. *Lancet*. 2015;386:1853–1860. doi: 10.1016/S0140-6736(15)00057-4.
11. Zimmermann FM, Ferrara A, Johnson NP, van Nunen LX, Escaned J, Albertsson P, Erbel R, Legrand V, Gwon HC, Remkes WS, Stella PR, van Schaardenburgh P, Bech GJ, De Bruyne B, Pijls NH. Deferral vs. performance of percutaneous coronary intervention of functionally non-significant coronary stenosis: 15-year follow-up of the DEFER trial. *Eur Heart J*. 2015;36:3182–3188. doi: 10.1093/eurheartj/ehv452.
12. Levine GN, Bates ER, Blankenship JC, Bailey SR, Bittl JA, Cercek B, Chambers CE, Ellis SG, Guyton RA, Hollenberg SM, Khot UN, Lange RA, Mauri L, Mehran R, Moussa ID, Mukherjee D, Nallamothu BK, Ting HH. 2011 ACCF/AHA/SCAI Guideline for Percutaneous Coronary Intervention: a report of the American College of Cardiology Foundation/American Heart Association Task Force on Practice Guidelines and the Society for Cardiovascular Angiography and Interventions. *Circulation*. 2011;124:e574–e651. doi: 10.1161/CIR.0b013e31823ba622.
13. Windecker S, Kolh P, Alfonso F. 2014 ESC/EACTS Guidelines on myocardial revascularization: the Task Force on Myocardial Revascularization of the European Society of Cardiology (ESC) and the European Association for Cardio-Thoracic Surgery (EACTS)Developed with the special contribution of the European Association of Percutaneous Cardiovascular Interventions (EAPCI). *Eur Heart J*. 2014;35:2541–2619. doi: 10.1093/eurheartj/ehu278.
14. Morris PD, van de Vosse FN, Lawford PV, Hose DR, Gunn JP. "Virtual" (computed) fractional flow reserve: current challenges and limitations. *JACC Cardiovasc Interv*. 2015;8:1009–1017. doi: 10.1016/j.jcin.2015.04.006.
15. Ntalianis A, Trana C, Muller O, Mangiacapra F, Peace A, De Backer C, De Block L, Wyffels E, Bartunek J, Vanderheyden M, Heyse A, Van Durme F, Van Driessche L, De Jans J, Heyndrickx GR, Wijns W, Barbato E, De Bruyne B. Effective radiation dose, time, and contrast medium to measure fractional flow reserve. *JACC Cardiovasc Interv*. 2010;3:821–827. doi: 10.1016/j.jcin.2010.06.006.
16. Tu S, Bourantas CV, Nørgaard BL, Kassab GS, Koo BK, Reiber JH. Image-based assessment of fractional flow reserve. *EuroIntervention*. 2015;11(suppl V):V50–V54. doi: 10.4244/EIJV11SVA11.
17. Morris PD, Ryan D, Morton AC, Lycett R, Lawford PV, Hose DR, Gunn JP. Virtual fractional flow reserve from coronary angiography: modeling the significance of coronary lesions: results from the VIRTU-1 (VIRTUal Fractional Flow Reserve From Coronary Angiography) study. *JACC Cardiovasc Interv*. 2013;6:149–157. doi: 10.1016/j.jcin.2012.08.024.
18. Papafaklis MI, Muramatsu T, Ishibashi Y, Lakkas LS, Nakatani S, Bourantas CV, Ligthart J, Onuma Y, Echavarria-Pinto M, Tsirka G, Kotsia A, Nikas DN, Mogabgab O, van Geuns RJ, Naka KK, Fotiadis DI, Brilakis ES, Garcia-Garcia HM, Escaned J, Zijlstra F, Michalis LK, Serruys PW. Fast virtual functional assessment of intermediate coronary lesions using routine angiographic data and blood flow simulation in humans: comparison with pressure wire - fractional flow reserve. *EuroIntervention*. 2014;10:574–583. doi: 10.4244/EIJY14M07_01.
19. Taylor CA, Fonte TA, Min JK. Computational fluid dynamics applied to cardiac computed tomography for noninvasive quantification of fractional flow reserve: scientific basis. *J Am Coll Cardiol*. 2013;61:2233–2241. doi: 10.1016/j.jacc.2012.11.083.
20. Tröbs M, Achenbach S, Röther J, Redel T, Scheuering M, Winneberger D, Klingenbeck K, Itu L, Passerini T, Kamen A, Sharma P, Comaniciu D, Schlundt C. Comparison of fractional flow reserve based on computational fluid dynamics modeling using coronary angiographic vessel morphology versus invasively measured fractional flow reserve. *Am J Cardiol*. 2016;117:29–35. doi: 10.1016/j.amjcard.2015.10.008.
21. Tu S, Westra J, Yang J, von Birgelen C, Ferrara A, Pellicano M, Nef H, Tebaldi M, Murasato Y, Lansky A, Barbato E, van der Heijden LC, Reiber JH, Holm NR, Wijns W; FAVOR Pilot Trial Study Group. Diagnostic accuracy of fast computational approaches to derive fractional flow reserve from diagnostic coronary angiography: the international multicenter FAVOR pilot study. *JACC Cardiovasc Interv*. 2016;9:2024–2035. doi: 10.1016/j.jcin.2016.07.013.
22. Huo Y, Kassab GS. Intraspecific scaling laws of vascular trees. *J R Soc Interface*. 2012;9:190–200. doi: 10.1098/rsif.2011.0270.
23. Molloi S, Wong JT. Regional blood flow analysis and its relationship with arterial branch lengths and lumen volume in the coronary arterial tree. *Phys Med Biol*. 2007;52:1495–1503. doi: 10.1088/0031-9155/52/5/018.
24. Takarada S, Zhang Z, Molloi S. An angiographic technique for coronary fractional flow reserve measurement: in vivo validation. *Int J Cardiovasc Imaging*. 2013;29:535–544. doi: 10.1007/s10554-012-0119-0.
25. Chen SJ, Carroll JD. 3-D reconstruction of coronary arterial tree to optimize angiographic visualization. *IEEE Trans Med Imaging*. 2000;19:318–336. doi: 10.1109/42.848183.
26. Messenger JC, Chen SY, Carroll JD, Burchenal JE, Kioussopoulos K, Groves BM. 3D coronary reconstruction from routine single-plane coronary angiograms: clinical validation and quantitative analysis of the right coronary artery in 100 patients. *Int J Card Imaging*. 2000;16:413–427.
27. Shechter G, Devernay F, Coste-Manière E, Quyyumi A, McVeigh ER. Three-dimensional motion tracking of coronary arteries in biplane cineangiograms. *IEEE Trans Med Imaging*. 2003;22:493–503. doi: 10.1109/TMI.2003.809090.
28. Yang Y, Zhu Q, Peng C, Wang H, Xue W, Lin G, Wen Z, Chang J, Wang M, Liu G, Li S. A novel approach for modelling vegetation distributions and analysing vegetation sensitivity through trait-climate relationships in China. *Sci Rep*. 2016;6:24110. doi: 10.1038/srep24110.
29. Seiler C, Kirkeeide RL, Gould KL. Basic structure-function relations of the epicardial coronary vascular tree. Basis of quantitative coronary arteriography for diffuse coronary artery disease. *Circulation*. 1992;85:1987–2003.
30. Tomasello SD, Costanzo L, Galassi AR. Quantitative coronary angiography in the interventional cardiology. In: Kirac S, ed. *Advances in the Diagnosis of Coronary Atherosclerosis*. Rijeka, Croatia: InTech; 2011:255–270.
31. Spaan JA. *Coronary Blood Flow: Mechanics, Distribution, and Control*. Netherlands: Springer; 1991.
32. Kirkeeide RL. Coronary obstructions, morphology physiologic significance. In: Reiber JHC, Serruys PW, eds. *Quantitative Coronary Arteriography.* Dordrecht: Kluwer Academy; 1991:229–244.
33. West GB, Brown JH, Enquist BJ. A general model for the origin of allometric scaling laws in biology. *Science*. 1997;276:122–126.
34. Wong JT, Le H, Suh WM, Chalyan DA, Mehraien T, Kern MJ, Kassab GS, Molloi S. Quantification of fractional flow reserve based on angiographic image data. *Int J Cardiovasc Imaging*. 2012;28:13–22. doi: 10.1007/s10554-010-9767-0.
35. Johnson NP, Kirkeeide RL, Asrress KN, Fearon WF, Lockie T, Marques KM, Pyxaras SA, Rolandi MC, van 't Veer M, De Bruyne B, Piek JJ, Pijls NH, Redwood S, Siebes M, Spaan JA, Gould KL. Does the instantaneous wave-free ratio approximate the fractional flow reserve? *J Am Coll Cardiol*. 2013;61:1428–1435. doi: 10.1016/j.jacc.2012.09.064.
36. Cook CM, Petraco R, Shun-Shin MJ, Ahmad Y, Nijjer S, Al-Lamee R, Kikuta Y, Shiono Y, Mayet J, Francis DP, Sen S, Davies JE. Diagnostic accuracy of computed tomography-derived fractional flow reserve: a systematic review. *JAMA Cardiol*. 2017;2:803–810. doi: 10.1001/jamacardio.2017.1314.

Validation Study of Image-Based Fractional Flow Reserve During Coronary Angiography

Mariano Pellicano, Ifat Lavi, Bernard De Bruyne, Hana Vaknin-Assa, Abid Assali, Orna Valtzer, Yonit Lotringer, Giora Weisz, Yaron Almagor, Panagiotis Xaplanteris, Ajay J. Kirtane, Pablo Codner, Martin B. Leon and Ran Kornowski

Circ Cardiovasc Interv. 2017;10:
doi: 10.1161/CIRCINTERVENTIONS.116.005259
Circulation: Cardiovascular Interventions is published by the American Heart Association, 7272 Greenville Avenue, Dallas, TX 75231

Print ISSN: 1941-7640. Online ISSN: 1941-7632

SUPPLEMENTAL MATERIAL

A Validation Study of Image-Based Fractional Flow Reserve (FFR_{angio}) During Coronary Angiography

Table I: Baseline characteristics per site

	Rabin Medical Center (105)	**Cardiovascular Center Aalst (73)**	**Columbia University Medical Center (8)**	**Shaare Zedek Medical Center (17)**
Age, mean ± SD	64.2 ± 9.9	68.5 ± 9.0	67.8 ± 9.1	65.5 ± 7.5
Male gender	68%	63%	75%	75%
Family history of CAD, %	29%	33%	57%	90%
Hypertension, %	63%	72%	100%	62%
Hypercholesterolemia, %	83%	86%	100%	81%
Diabetes, %	40%	17%	50%	25%
Smoking (current), %	23%	9%	13%	19%
Smoking (prior), %	26%	17%	13%	31%
Prior MI, %	23%	11%	25%	25%
Prior PCI, %	39%	32%	50%	25%
Stable angina, %	52%	83%	75%	75%
Unstable angina %	31%	9%	25%	19%
NSTEMI, %	15%	8%	0%	7%
Radial access, %	78%	65%	63%	94%
Femoral access, %	22%	35%	37%	6%

Table II: Mean FFR and FFR_{angio} measurements by site

Site	FFR	FFR_{angio}
Rabin Medical Center	0.84	0.84
Cardiovascular Center Aalst	0.75	0.78
Columbia University Medical Center	0.88	0.86
Shaare Zedek Medical Center	0.83	0.83

Table III: Linear regression by site

Site (patients)	r
Rabin Medical Center (105)	0.90
Cardiovascular Center Aalst (73)	0.86
Columbia University Medical Center (8)	0.92
Shaare Zedek Medical Center (17)	0.66

Table IV: Linear regression and Bland Altman analysis by minimum and maximum FFR invasive measurement

	Minimum FFR invasive	Maximum FFR invasive
r	0.877	0.879
Estimated bias (mean difference ± SD)	0.0127	0.0075
95% limits of agreement	-0.101 to +0.126	-0.106 to +0.121

Figure I. ROC curve for predicting invasive FFR at 0.80.